Article Title: Adapting C_4 photosynthesis to atmospheric change and increasing productivity by elevating Rubisco content in Sorghum and Sugarcane.

Authors and Affiliations:

Coralie E. Salesse-Smith[1,3], Noga Adar[1], Baskaran Kannan[4,5], Thaibinhduong Nguyen[4,5], Ming Guo[6,7], Zhengxiang Ge[6,7], Fredy Altpeter[4,5], Tom E. Clemente[6,7], and Stephen P. Long[1,2,3]

[1]Carl R. Woese Institute for Genomic Biology, University of Illinois at Urbana-Champaign, Urbana, IL, USA; [2]Departments of Plant Biology and of Crop Sciences, University of Illinois at Urbana-Champaign, Urbana, IL, USA; [3]DOE Center for Advanced Bioenergy and Bioproducts Innovation, Urbana-Champaign, IL, USA; [4]Agronomy Department, Plant Molecular and Cellular Biology Program, Genetics Institute, University of Florida, IFAS, Gainesville, Florida, USA; [5]DOE Center for Advanced Bioenergy and Bioproducts Innovation, Gainesville, FL, USA; [6]Department of Agronomy and Horticulture, University of Nebraska-Lincoln, Lincoln, NE, USA; [7]DOE Center for Advanced Bioenergy and Bioproducts Innovation, Lincoln, NE, USA

Corresponding authors:

Coralie E. Salesse-Smith, ces343@illinois.edu

Stephen P. Long, slong@illinois.edu

Classification:

Biological Sciences, Plant Biology

Keywords: Atmospheric change; Future-proofing agriculture; Rising CO_2; Rubisco, C_4 photosynthesis, Bundle sheath leakiness; Photosynthetic induction; CO_2 assimilation, RAF1, Transgenic field trial, Sorghum, Sugarcane

Abstract

Meta-analyses and theory show that with rising atmospheric [CO_2], Rubisco has become the greatest limitation to light-saturated leaf CO_2-uptake (A_{sat}) in C_4 crops. So would transgenically increasing Rubisco increase A_{sat} and result in increased productivity in the field? Here, we successfully overexpressed the Rubisco small subunit (RBCS) with Rubisco accumulation factor 1 (RAF1) in both sorghum and sugarcane, resulting in significant increases in Rubisco content of 13-25% and up to 90% respectively. A_{sat} increased 12-15% in three independent transgenic events of both species. Sorghum plants also showed increased speeds of photosynthetic induction and decreased bundle sheath leakiness. These improvements translated into average increases of 15.5% in biomass in field-grown sorghum and a 37-81% increase in greenhouse-grown sugarcane. This suggests a potential opportunity to achieve substantial increases in productivity of this key economically important clade of C_4 crops, future proofing their value under global atmospheric change.

Significance Statement

The world is projected to need a 60% increase in food supply by 2050 (UN), and this must be achieved under conditions of global change without expanding onto yet more land. C_4 crops, while few in number, account for a large proportion of agricultural productivity. We reason that rising atmospheric [CO_2] has very recently made Rubisco, the enzyme used for all carbon fixation in plants, the greatest limitation to light saturated photosynthesis in C_4 crops. We demonstrate that transgenically increasing Rubisco content in sorghum and sugarcane, increases their photosynthetic efficiency and productivity, including in a field trial of sorghum. This shows a means to sustainably increase the productivity of this key group of crops.

67 **Introduction**

68 While very few of the 161 crop species listed by UN-FAO use C_4 photosynthesis, their
69 importance and potential in terms of global food, feed and biomass production is exceptional[1].
70 For total global biomass harvested, sugarcane (*Saccharum* hybrids) is number one and maize
71 (*Zea mays* L.) number one for seed harvested[1,2]. Sorghum (*Sorghum bicolor*) is the fourth most
72 important cereal in global production, only behind, maize, rice and wheat, but it is the major
73 cereal of the semi-arid tropics [1]. While grown for biomass, the C_4 crops energycane and
74 Miscanthus show exceptional productivity[3-6]. These crops all belong to the monophyletic grass
75 tribe Andropogonae.

76 The leaves of C_4 plants contain an outer layer of mesophyll cells surrounding the bundle sheath
77 cells. CO_2 diffuses from the sub-stomatal cavity into the mesophyll cytoplasm, where it
78 combines with phosphoenolpyruvate (PEP) to form oxaloacetate (OAA), catalyzed by
79 cytoplasmic PEP carboxylase (PEPC). OAA is reduced to malate in the mesophyll chloroplasts
80 and then diffuses to the bundle sheath where it is decarboxylated by $NADP^+$-dependent malic
81 enzyme (NADP-ME) creating a high [CO_2] around Ribulose-1:5 bisphosphate
82 carboxylase/oxygenase (Rubisco). The decarboxylation product, pyruvate, diffuses back to the
83 mesophyll where, catalyzed by Pyruvate Pi dikinase (PPDK), it is phosphorylated to PEP at the
84 expense of 2ATP, completing the photosynthetic C_4 cycle[7]. This photosynthetic C_4 cycle is in
85 effect a light energy driven CO_2 pump that elevates the [CO_2] around Rubisco to a level that is
86 sufficient to competitively inhibit oxygenation, preventing photorespiration and avoiding the
87 significant losses of photosynthetic efficiency that this causes in C_3 species[8]. Its benefits are
88 such that considerable effort is being placed into engineering the C_4 pathway into C_3 crops[9-11].
89 Tests under open-air conditions using Free-Air Concentration Enrichment (FACE) technology,
90 have shown that higher [CO_2] increases the photosynthetic efficiency, and in turn productivity,
91 of C_3 crops, but not these C_4 crops [12-16]. Thus, rising atmospheric [CO_2] could progressively
92 erode the current production advantage of C_4 plants[17]. However, analysis of metabolic and
93 physiological limitations indicate that C_4 plants could be modified to also gain photosynthetic
94 efficiency at today's and future atmospheric [CO_2] [18-20].

95 Light-saturated leaf CO_2 uptake (A_{sat}) in C_4 plants rises sharply with intercellular CO_2
96 concentration (C_i) to a plateau, where A_{sat} remains constant with further increase in C_i [7]. In
97 maize crops grown in the field at both ambient and elevated atmospheric CO_2, this transition
98 was shown to occur at a C_i of about 120 µmol mol^{-1}, above which A_{sat} is [CO_2]-saturated [15]. A
99 meta-analysis of 842 measured A-C_i responses in 49 C_4 species showed the point of CO_2
100 saturation is consistent across a broad range of C_4 species, and unaffected by growth at either
101 sub-ambient or supra-ambient [CO_2] [19]. Because of their lower stomatal conductance (g_s)
102 relative to A_{sat}, the drawdown of [CO_2] between the atmosphere (C_a) and intercellular air space
103 (C_i) is greater in C_4 leaves, resulting in a ratio (C_i/C_a) of about 0.4, compared to 0.7 in C_3 species.

These ratios in non-water stressed plants are apparently unaffected by the [CO_2] of the growth environment [12]. At today's C_a of 428 µmol mol^{-1} [21], C_i in photosynthesizing C_4 leaves should be about 170 µmol mol^{-1}. Therefore, at current and future atmospheric [CO_2], C_4 photosynthesis is [CO_2] saturated. Historically this was not the case. The average C_a of the last 40,000 years in which our crop ancestors evolved was 220 µmol mol^{-1} and assuming a C_i/C_a, of 0.4 under these conditions average C_i would have been 88 µmol mol^{-1}, well below the indicated saturation point of about 120 µmol mol^{-1} [12,22]. At this C_i photosynthesis would be operating on the initial slope of the response of A to C_i. The mechanistic steady-state mathematical model of C_4 photosynthesis shows that this initial slope is determined by the activity of PEPC and mesophyll conductance (g_m); g_m being the ease with which CO_2 can diffuse from the sub-stomatal cavity into the mesophyll cytoplasm[7]. The plateau however, is limited by the activity of Rubisco, and potentially electron transport[7]. Recent non-steady state metabolic modeling and measurements show Rubisco activity also having significant control over the efficiency of photosynthesis in fluctuating light [23,24]. Consistent with these predictions, transgenic knock-down studies showed metabolic control of the initial slope of the A-C_i response to reside with PEPC activity and the plateau shared by Rubisco and PPDK, with Rubisco accounting for 70% of the control [25]. This indicates that up-regulation of Rubsico would increase A_{sat} in today's elevated [CO_2] atmosphere.

Form I Rubisco, found in plants, is made up from eight small subunits (SS) encoded by the nuclear gene family *RBCS* and eight large subunits (LS) encoded by the chloroplast gene *rbcL*. Previously, transgenic increase in Rubisco content, by overexpression of the Rubisco small-subunit (*RBCS*) and Rubisco accumulation factor 1 (*RAF1*) genes, increased A_{sat} and plant growth of maize under optimal and chilling growth conditions [26,27]. However, this was confined to a single hybrid genotype of maize grown in controlled environments. To test the hypothesis that this improvement would be more generally possible across this key economic clade of crops and result in increased productivity in the field and greenhouse, Rubisco was up-regulated in both sorghum and sugarcane.

Results

Transgenic overexpression of RBCS and RAF1 increases Rubisco abundance in sorghum and sugarcane

Two transgenes, each designed to upregulate RBCS and RAF1, were stably transformed into sorghum and sugarcane (Fig.1a). The construct transformed into sorghum contains constitutive promoters, while the one transformed into sugarcane contains bundle sheath specific promoters as well as C-terminal epitope tags FLAG and HA. Three independent events were obtained for each species and wild-type (WT), from which the transformants were derived, propagated alongside these. In sorghum, homozygous plants were obtained from each single

141 insertion event (hn1a, zg12a and zg5b) at T2. Commercial sugarcane is clonally propagated,
142 and the three events (3, 9, and 25) were effectively clones of the T0 events.

143 qPCR confirmed transgene expression in sorghum lines characterized in both the greenhouse
144 and field. All three transgenic events showed high levels of *ZmRBCS* and *ZmRAF1* expression,
145 with none in the WT (Fig. S1a-d). Immunoblots similarly showed high RAF1 protein expression
146 in the transgenic lines relative to WT (Fig. 1b). Epitope tags showed expression of sorghum SS
147 and RAF1 proteins in the sugarcane transformants (Fig. 1c).

148 Rubisco content, measured by the ^{14}C-CABP binding assay, was significantly increased by 13-
149 25% in sorghum, and by 90% and 39% in sugarcane events 3 and 25 respectively (Fig. 1d,e). No
150 significant increase was measured in event 9, even though immunoblots showed the presence
151 of the recombinant SS and RAF1, although the latter at lower levels than in events 3 and 25 (Fig.
152 1c). There were no differences in total soluble protein between WT and transgenic plants in
153 either sorghum or sugarcane (Table S2).

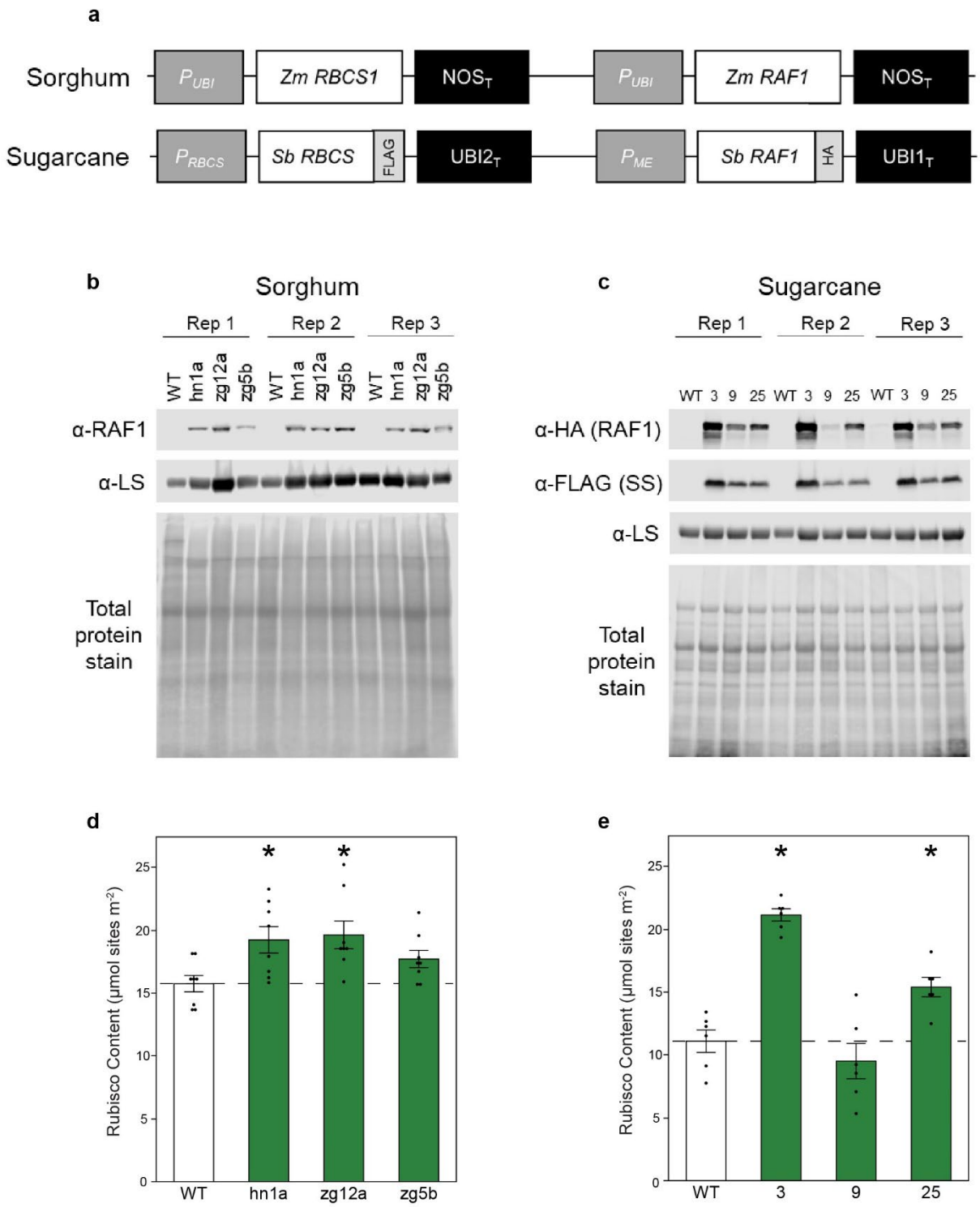

Fig. 1: Sorghum and sugarcane transformation constructs, protein expression and analysis of Rubisco content.

(a) Transgenes designed to upregulate Rubisco small subunit (SS) and Rubisco accumulation factor 1 (RAF1). The transgenes were stably transformed into sorghum (top) and sugarcane (bottom). Sb, *Sorghum bicolor*; Zm, *Zea*

158 *mays*. **(b)** Total soluble protein isolated on a leaf area basis from sorghum and **(c)** sugarcane, and analyzed by
159 immunoblot. Three replicate plants (Rep) of each of the three transgenic events and of the wildtype (WT) control
160 were probed with antibodies indicated to the left. **(d)** Average Rubisco content per unit leaf area quantified by ^{14}C-
161 CABP binding in 6-week-old sorghum (n=8), and **(e)** 9-week-old sugarcane (n=6) grown in the greenhouse. Values
162 are shown as the mean ± SEM. Asterisks indicate significant differences between WT and the transgenic line (*P <
163 0.05); one-way ANOVA, Dunnett's post hoc test.

164

165 **Co-upregulation of RBCS and RAF1 is correlated with increased $V_{c,max}$, CO_2 assimilation, and**
166 **photosynthetic light induction in sorghum**

167 *A*-C_i responses showed that upregulated RBCS and RAF1 significantly increased assimilation
168 rates above a C_i of ~100 µmol mol $^{-1}$, but not below (Fig. 2a). Maximum *in vivo* Rubisco
169 carboxylation rates ($V_{c,max}$) at 25 °C, estimated from the *A*-C_i response, were significantly
170 increased by 12% in the transgenic lines (Fig 2b), while maximum PEPC carboxylation rates
171 ($V_{p,max}$) did not differ (Table 1). A_{sat} measured at the current atmospheric [CO_2] was similarly
172 increased in the transgenic lines (Fig. 2c). g_{sw} also increased in concert with A_{sat} such that no
173 differences in C_i were observed between genotypes (Table 1). The effective quantum yield of
174 PSII (Φ_{PSII}), measured by modulated chlorophyll fluorescence, was increased by 12% in the
175 transformed plants in parallel with CO_2 assimilation (Table 1).

176 To identify if increased Rubisco would be beneficial to the activation of photosynthesis on
177 shade to sun transition, induction of *A* over the first 30 min of transfer to high-light (PPFD =
178 1800 µmol m^{-2} s^{-1}) was measured (Fig. 2d). CO_2 assimilation in the transgenic lines was
179 significantly higher than WT after 3 minutes of illumination following dark acclimation (Fig. 2e)
180 and remained higher for the remaining 27 minutes of measurement (Fig. 2d). Induction curves,
181 normalized to the average *A* value over the last 5 minutes of illumination (A_{max}) were used to
182 assess the speed of photosynthetic activation (Fig. S2a). On average, the transgenics took 4
183 minutes to reach 50% maximum CO_2 assimilation rates (A_{max}), compared to 6 minutes for WT
184 (Fig. 2f). The transgenics were significantly taller and had more leaves than WT in the
185 greenhouse (Fig. S3). Seed from these plants was collected for the field trial.

186

187

188

189

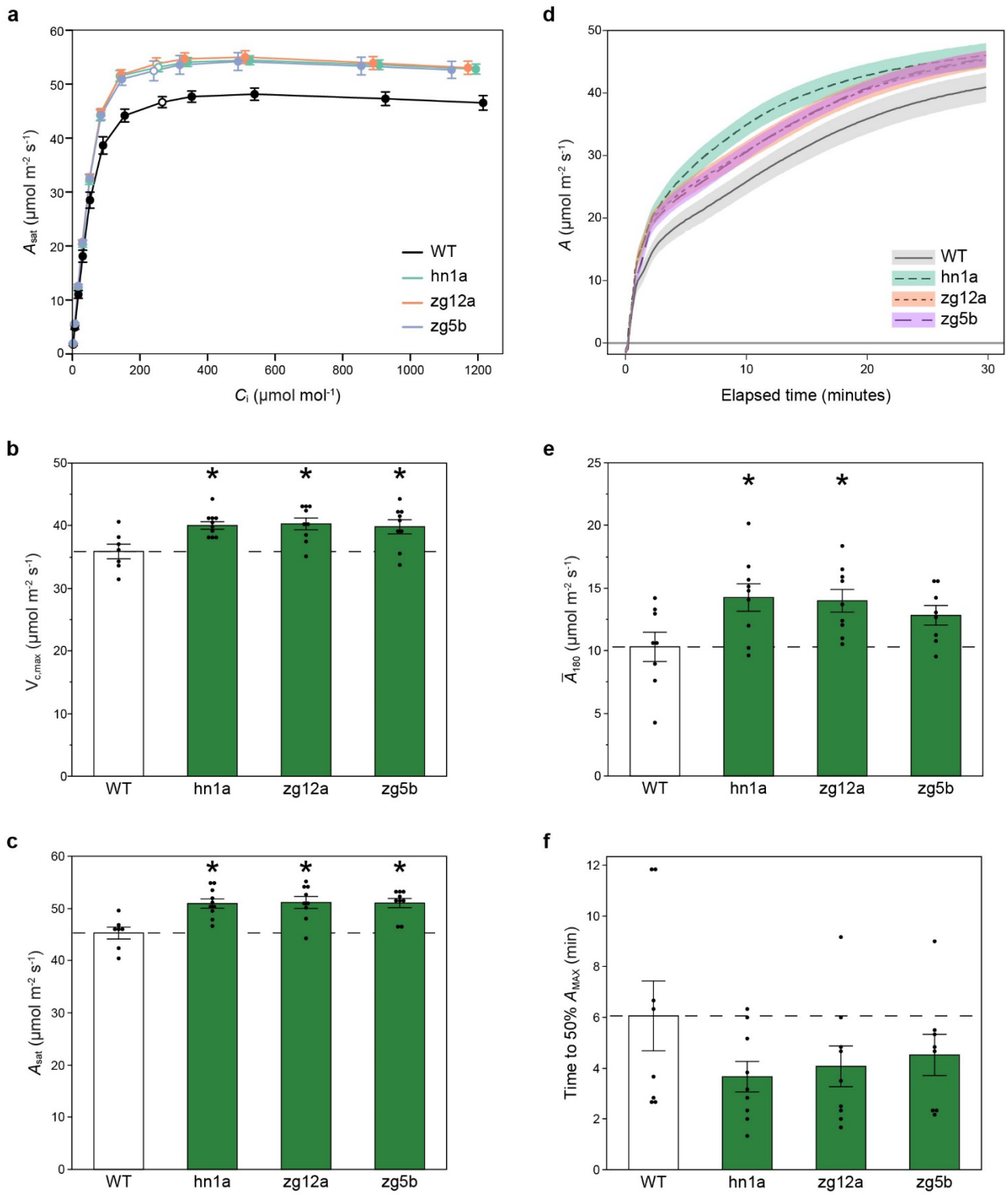

Fig 2: CO_2 response curves and photosynthetic induction to light of greenhouse grown sorghum plants.

(a) Response of net CO_2 assimilation (A_{sat}) to intercellular [CO_2] (C_i). Measurements were made under the following conditions: light intensity of 1800 µmol m^{-2} s^{-1}, leaf temperature of 28 °C, and VPD 1.5 kPa. Measurement cuvette

[CO_2] were varied from 10-1500 µmol mol^{-1} CO_2. Open points represent the measured value closest to the operating C_i (i.e the Ci where ambient CO_2 was 420 µmol mol^{-1}). **(b)** Maximum *in vivo* Rubisco carboxylation rate ($V_{c,max}$) at 25 °C estimated from response curves in panel **a**. **(c)** A_{sat} measured at 400 µmol mol^{-1} CO_2 **(d)** Induction of net CO_2 assimilation during the first 30 min of illumination at PPFD 1800 µmol m^{-2} s^{-1}. **(e)** Average CO_2 assimilation during the first 180 seconds of induction. **(f)** Time for A to reach 50% of $A_{max,}$ where A_{max} is the average A from 25 to 30 minutes of illumination. Measurements were made on 5-week-old plants. Values are shown as the mean ± SEM (n =7-10). Asterisks indicate significant differences between WT and the transgenic line (*P < 0.05); one-way ANOVA, Dunnett's post hoc test.

RBCS-RAF1 transgenic sorghum plants have increased photosynthesis and biomass under field conditions

A field trial in summer 2023 evaluated whether gains observed in the greenhouse could be reproduced in a replicated field trial of 4-row plots. A randomized complete block design was used with 6 replicate plots for each of the three RBCS-RAF1 transgenic events and WT (Fig. 4d; Fig. S4a). A-C_i responses and light induction curves measured during the vegetative growth stage were consistent with the greenhouse results. $V_{c,max}$, was again increased, with no increase in the initial slope of the response, and light induction of A was faster (Fig 3a,b). These increases were also observed at boot stage but were absent during grain-filling (Fig. 3c,d). Bundle sheath leakiness (Φ), the rate that CO_2 not fixed by Rubisco leaks from bundle sheath back to mesophyll, was measured by combining gas exchange with carbon isotope discrimination during the vegetative growth stage. In concert with increased $V_{c,max}$, Φ was decreased by about 18% across all three transgenic lines (Fig. S5).

The field grown transgenic sorghum plants were also more vigorous than the WT, as evidenced by a significant 15.5% increase in vegetative dry biomass at harvest (Fig. 4a). However, there was no increase in seed biomass, which corresponded to a significant decrease in harvest index (seed mass/total plant mass) compared to the WT (Fig. 4b-c). Leaf mass, chlorophyll content, N and C contents, on a leaf area basis, did not differ between the WT and transgenic plants (Table S2).

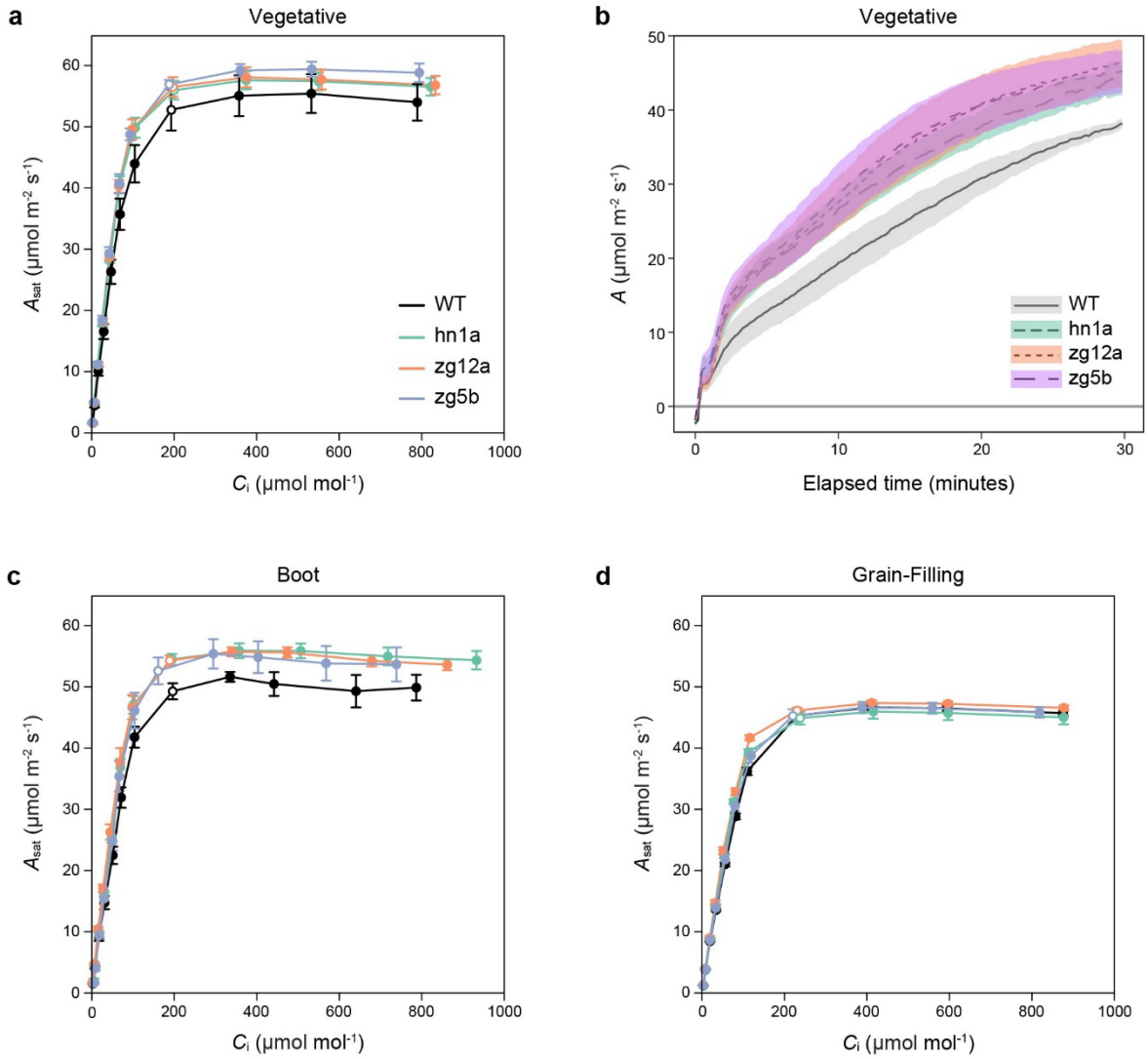

Fig. 3: CO_2 response curves and photosynthetic induction to light of field grown sorghum plants.

(a) Response of light-saturated CO_2 uptake (A_{sat}) to intercellular [CO_2] (C_i) and **(b)** induction of A during the first 30 min of illumination at PPFD 1800 µmol m^{-2} s^{-1} of sorghum plants in the vegetative growth stage. **(c)** A_{sat} - C_i response of sorghum plants in the boot and **(d)** grain-filling growth stages. Open symbols on each curve show the measured value closest to the operating C_i (where ambient CO_2 is 420 µmol mol^{-1}). Values are shown as the mean ± SEM (n =4-6).

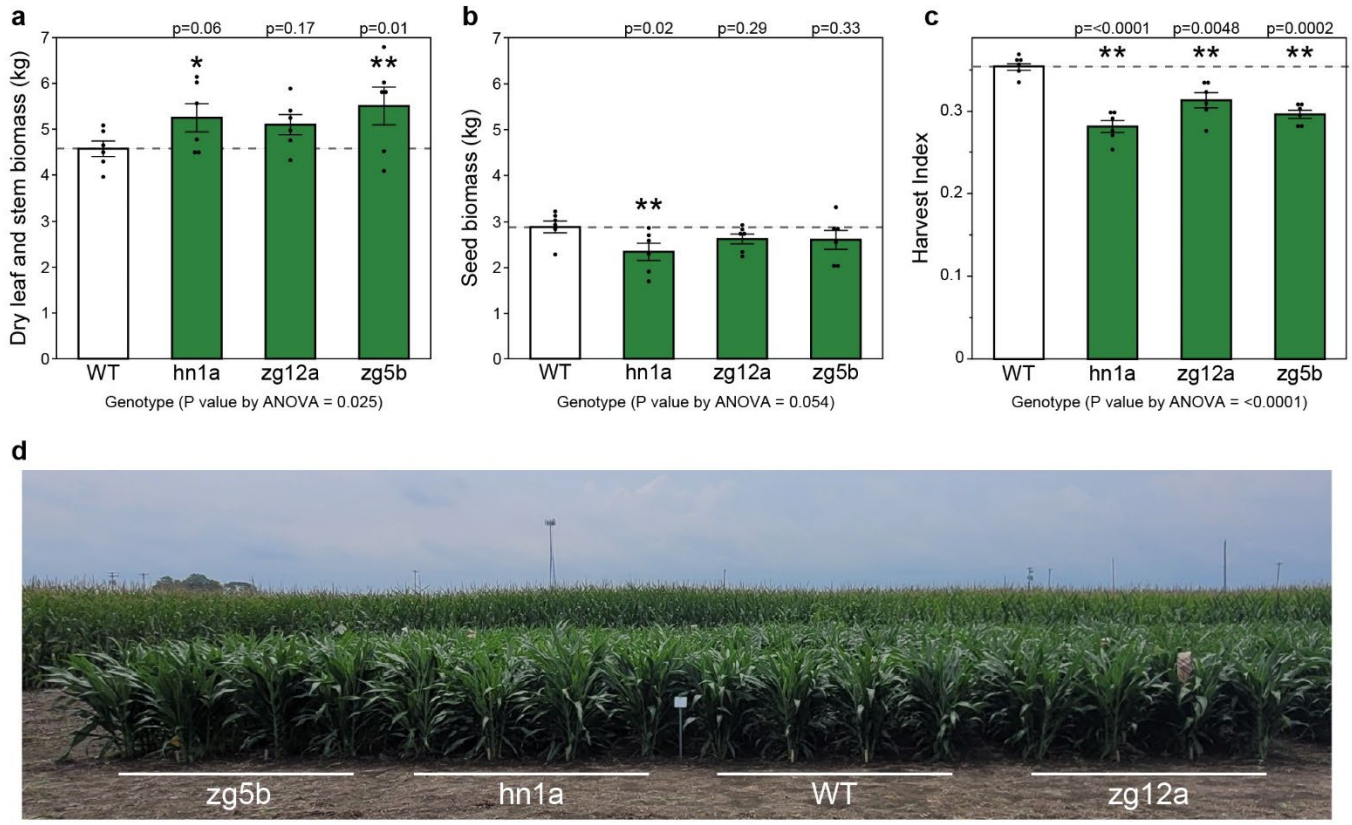

Fig. 4: Plant growth traits in field grown sorghum plants.

(**a**) Average dry leaf and stem biomass per plot and **(b)** average seed biomass per plot from field grown sorghum plants. **(c)** Harvest index (seed mass/total shoot mass) per plot. Values are shown as the mean ± SEM (n = 6 plots). Asterisks indicate significant differences between WT and the transgenic line (**P < 0.05, *P < 0.1); one-way ANOVA, Dunnett's post hoc test. P values above each bar from Dunnett's post hoc test. **(d)** Side view of 4 of the 24 four-row plots of the four sorghum genotypes tested at boot stage in the field in Urbana, Illinois summer 2023 (see Fig. S4a for full experimental design).

Co-upregulation of RBCS and RAF1 in sugarcane increases photosynthetic efficiency and plant productivity

Measurements were made on 8-week-old greenhouse grown sugarcane plants. As in sorghum, A-C_i responses showed significant increases in *in vivo* Rubisco activity ($V_{c,max}$) with no change in the initial slope ($V_{p,max}$, Fig. 5a,c; Table 1). Similarly, A_{sat} was significantly increased at ambient atmospheric [CO_2] in the transgenics (Fig. 5d). There were no significant differences in g_{sw} or C_i: however, there was a marginal increase in Φ_{PSII} in events 3 and 25 (Table 1). Assimilation of CO_2 was greater over the 30 minute light induction, in events 3 and 25, but not event 9 (Fig. 5b, Fig. S6).

Transgenic events 3 and 25 showed significant increases in main stem, and tiller and leaf dry mass, amounting to total shoot dry mass increases of 37% and 81% respectively, but with no increase in event 9 (Fig. 5e-g). Significant increases in plant height, stem width and leaf number were also observed in events 3 and 25 compared to WT (Fig. S7). Leaf chlorophyll and mass per unit area did not differ between genotypes (Table S2).

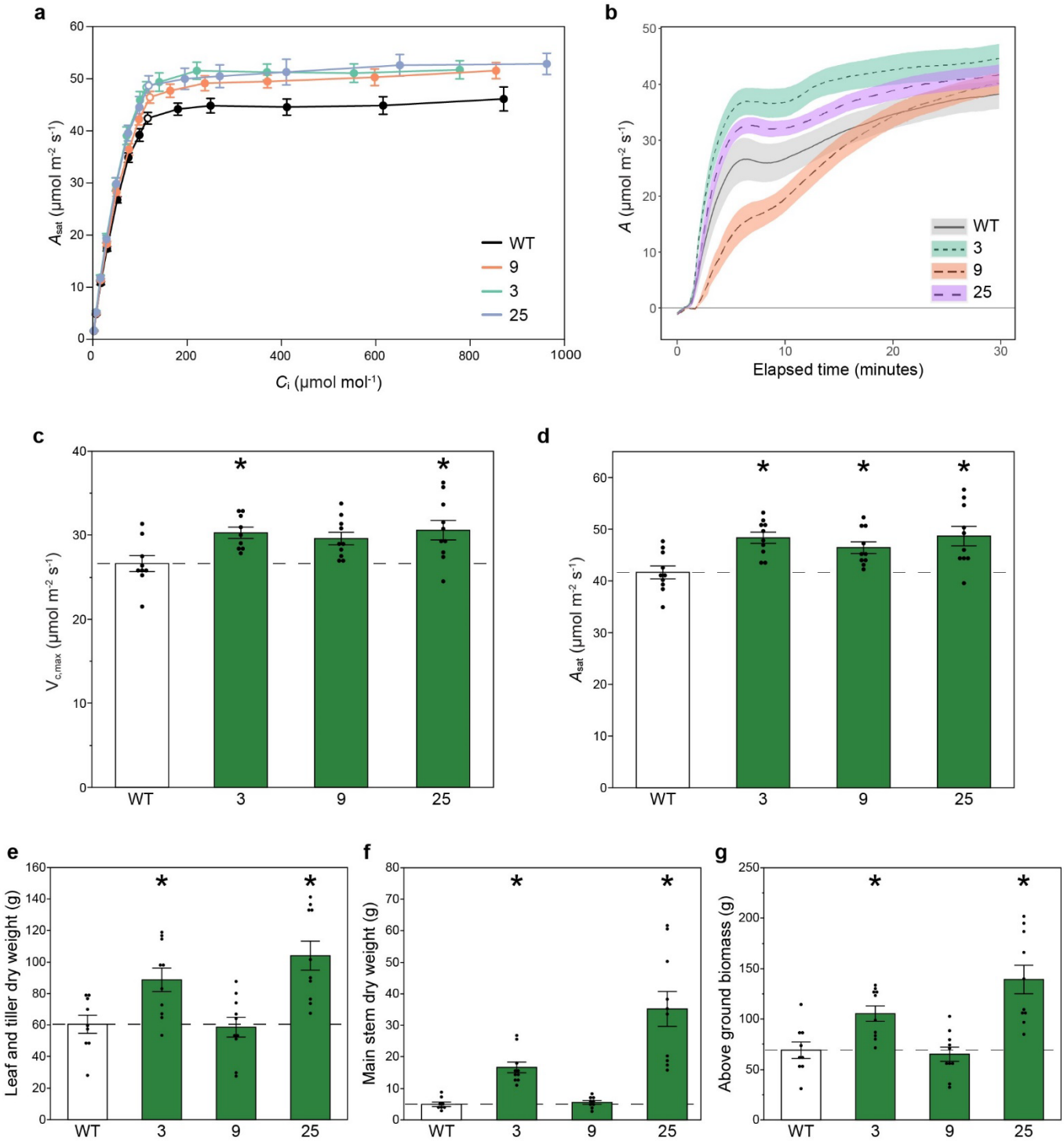

Fig 5: CO_2 response curves and plant growth traits of greenhouse grown sugarcane plants.

(a) Response of light-saturated CO_2 uptake (A_{sat}) to intercellular [CO_2] (C_i). Measurements were at light intensity of 1800 µmol m^{-2} s^{-1}, leaf temperature 30 °C, and 65% humidity. Measurement cuvette [CO_2] was varied from 10-1500 µmol mol^{-1}. Open symbols show the measured value closest to the operating C_i (where ambient [CO_2] was 420 µmol mol^{-1}). **(b)** Induction of A during the first 30 min of illumination at PPFD 1800 µmol m^{-2} s^{-1}. **(c)** Maximum

Rubisco carboxylation rate *in vivo* ($V_{c,max}$) at 25 °C estimated from response curves in panel **a**. **(d)** A_{sat} at 450 µmol mol^{-1} CO_2 **from panel a (e)** Leaf and tiller, **(f)** main stem, and **(g)** above ground total dry biomass of greenhouse grown sugarcane plants. Values are shown as the mean ± SEM (n =8-10). Asterisks indicate significant differences between WT and the transgenic lines (*P < 0.05); one-way ANOVA, Dunnett's post hoc test.

Discussion

Theoretical and experimental analyses have long suggested Rubisco to be the major limitation of light-saturated photosynthesis in both C_3 and C_4 species[7,18-20,28]. Consistent with this hypothesis, transgenic up-regulation of Rubisco content significantly increased light-saturated leaf CO_2 uptake (A_{sat}) in both sorghum and sugarcane (Fig. 2a-c, 3a-c, and 5a-d). The speed of light induction of CO_2 uptake rate was also increased (Fig. 2d-f and 3b). This has critical importance to increasing photosynthetic efficiency under the fluctuating light conditions of crop canopies in the field[29,30]. Also consistent with limitation by Rubisco, bundle sheath leakiness was decreased (Fig. S5). Finally, and in concert with these increases in photosynthetic efficiency, a field trial of sorghum and a greenhouse trial of sugarcane showed significant increases in productivity relative to the wild-type from which the transgenics were derived (Figs. 4 and 5).

Rubisco is, by far, the most abundant single protein in leaves, constituting up to 50% of soluble protein in C_3 plants and 20-30% in C_4[31]. These high amounts are attributed to the need to offset the exceptionally low catalytic rate of carboxylation (k_{cat}) of Rubisco relative to other enzymes. Its low k_{cat} is in turn considered in part a consequence of high specificity for CO_2 relative to the alternative substrate of O_2[32]. Sage & McKown[33] noted the much lower available tissue volume that could house Rubisco in C_4 leaves, where it is functionally confined to the bundle sheath, suggesting this as a constraint. This is less than half the volume available in C_3 leaves. However, 3D microscopic analysis of the bundle sheath chloroplast stromal volume in *Miscanthus* x *giganteus* suggested capacity for a doubling of actual Rubisco content[34]. *Miscanthus* is closely related to sorghum and sugarcane, and within the same subtribe, Saccharinae[35]. This observation is consistent with the observed increases in Rubisco content of 25% in sorghum and up to 90% in sugarcane (Fig. 1d-e). The much higher level in sugarcane may reflect that this was achieved by biolistic transformation, which could have resulted in multiple insertions of the transgenes, while the three sorghum events were single insertion events.

Given that increased Rubisco production is possible and beneficial, why have natural selection and breeding not achieved this? One explanation is that Rubisco might only have become a limitation very recently, due to rising atmospheric [CO_2]. On March 16, 2024, atmospheric [CO_2] was recorded at 428 µmol mol^{-1} [21], which is almost double the average atmospheric [CO_2] of the past 40,000 years [22,36]. Theory suggests that under the conditions in which our crop ancestors evolved, Rubisco would not be a limitation and therefore selection pressure would have been

300 lacking, with the result that there may be little genetic variation for natural or breeder selection
301 as [CO_2] rises. Indeed given the large nitrogen cost of Rubisco, historically, selection pressure
302 was likely against any increase. It should be noted that half of the increase in [CO_2] has occurred
303 in the last 50 years, with [CO_2] rising from 323 µmol mol^{-1} to 428 µmol mol^{-1} between 1974 and
304 2024 [21]. By reference to the open symbols in Fig. 3, it is seen that at today's atmospheric [CO_2]
305 A_{sat} in the field-grown sorghum is controlled by the plateau of the A-C_i response, i.e.
306 predominantly by Rubisco activity. However, if it is assumed that C_i/C_a has been conserved,
307 then at the atmospheric [CO_2] in 1974, C_i would equal 129 µmol mol^{-1}. By reference to Fig. 3,
308 A_{sat} would then be mostly controlled by the initial slope of the A-C_i response, i.e. PEP
309 carboxylase activity ($V_{p,max}$), and insensitive to increase in Rubisco activity. The period in which
310 Rubisco has become limiting is therefore very short in terms of reproductive cycles. As
311 atmospheric [CO_2] continues to rise, Rubisco limitations will increase, and elevation of Rubisco
312 will be an important means to contribute toward future-proofing and advancing C_4 crop
313 productivity.

314 An increase in A_{sat} was achieved here by only up-regulating expression of *RBCS* and *RAF1,* which
315 infers three factors important for future manipulations. First, for Rubisco to be increased, both
316 the large (LS) and small (SS) sub-units, must be increased. That only up-regulation of *RBCS* was
317 needed, is consistent with the observations that *rbcL* is subject to assembly-dependent
318 translational regulation, and so controlled by the supply of SS [37]. Second, although all three
319 transgenic sugarcane events showed expression of the SbRBCS protein, in event 9 this did not
320 translate into improved productivity (Fig. 1c-e and 5e-g). Expression of SbRAF1 was lowest in
321 this line, suggesting the importance of effective expression of RAF1 with RBCS (Fig.1c). Third,
322 there must either be 1) over-capacity in the C_4 cycle or 2) the C_4 cycle increases capacity in
323 concert with increased Rubisco activity. The fact that bundle sheath leakiness of CO_2 decreased
324 and $V_{p,max}$ did not increase with increased Rubisco is consistent with hypothesis 1[24].

325 In dense modern crop canopies, only the uppermost leaves might experience light saturated
326 conditions. Most leaves will experience frequent light fluctuations, or sunflecking, due to the
327 passage of clouds, shadowing by overlying leaves as solar angle changes and wind driven
328 movements[29,30]. The speed with which photosynthetic efficiency can adjust to light fluctuations
329 has been shown to have a profound effect on whole crop daily CO_2 assimilation and
330 productivity[38,39]. A key factor here is the speed of induction of A on transfer of a leaf from
331 shade to sun. Modeling and experimental studies have shown the speed at which Rubisco
332 activity increases to be critical to induction in both C_3 and C_4 crops[23,40,41]. Here, increased
333 Rubisco content coincided with more total CO_2 assimilation over the 30 minutes of induction in
334 all three sorghum events and two of the sugarcane events. Activation of Rubisco requires the
335 chaperone protein Rubisco activase (RCA), suggesting that these events must have had
336 sufficient RCA to support the activation of their additional Rubisco (Fig. 2d, 3b, 5b).

337 In the greenhouse, significant increases in growth of both sorghum and sugarcane were
338 observed at an individual plant level (Fig. 5e-g; Fig. S3). Importantly, and consistent with
339 increased CO_2 assimilation rates during vegetative and boot stages, leaf and stem biomass was
340 significantly increased by an average of 15.5% in the RBCS-RAF1 sorghum field plots relative to
341 the WT controls, a desired characteristic for C_4 biomass crops (Fig. 4a). However, grain yield per
342 plot did not increase, due to a significant decrease in harvest index (Fig.4c). Although sorghum
343 cultivar RTx430 has become the standard for transformation and experimental analyses, it is a
344 40-year old inbred line[42-44] and might be sink-limited. Sink limitation at grain filling results in
345 accumulation of non-structural carbohydrates in the source tissues, causing down-regulation of
346 photosynthetic genes, notably *RBCS* [45]. The loss of *in vivo* Rubisco activity ($V_{c,max}$) during grain
347 filling evident in Fig. 3 is consistent with sink limitation. Testing whether greater grain yields can
348 be obtained will require the production of hybrids and/or transformation of current elite
349 cultivars. Up-regulation of Rubisco has been achieved here, as a test of the concept that more
350 Rubisco would translate to more efficient photosynthesis and productivity in today's
351 atmosphere, by addition of extra copies of *RBCS* and *RAF1.* Alternatively, a future approach for
352 upregulating Rubisco could be using DNA editing to mutate repressive elements in the
353 promoter regions of the native *RBCS* and *RAF1* genes.

354 Despite significant breeding efforts, the average yield of sorghum has not changed over 30
355 years, nor has the yield of sugarcane in the USA in the last 20 years (Fig. S8a,b). This might
356 reflect increasingly adverse weather conditions. However, even in the USA where it might be
357 assumed that favorable agronomy would allow the yield potential to be realized, there is little
358 evidence of yield improvement since 1991, even in the most favorable years (Fig. S8a).
359 Therefore, if the photosynthetic and productivity improvements found here by up-regulating
360 Rubisco translate into parallel yield improvements in elite cultivars and hybrids, this could be
361 very useful for integration into breeding programs. This successful test-of-concept suggests
362 multi-location and/or multi-year replicated yield trials of Rubisco up-regulation in elite material
363 as the next proving step. Given the great value and global significance of this key economic
364 clade of crops both for food and biomass, the results here indicate an important opportunity to
365 achieve increased productivity under rising atmospheric [CO_2].

366

367 **Methods**

368 **Sorghum plasmid assembly and transformation**

369 A 3.6 kb fragment containing the Raf1 expression cassette regulated by the maize ubiquitin
370 promoter was isolated from the plasmid pPTN1063[26] by digesting the vector with *Kpn*I and
371 *Hind*III. The fragment was then blunted with T4 DNA polymerase and ligated with a linearized
372 pPTN438[37] (containing the RBCS expression cassette), via *Kpn*I digestion and blunted with T4

373 DNA polymerase, resulting in the final binary vector pPTN1589. Sorghum inbred RTx430 was
374 transformed using agrobacterium as previously described[46].

375

376 **Sugarcane plasmid assembly**

377 Recombinant DNA constructs were assembled with Golden Gate cloning to highly express
378 Rubisco small subunit (*RBCS*) and Rubisco accumulation factor 1 (*RAF1*) from *Sorghum bicolor* in
379 sugarcane. The open reading frame (ORF) of *SbRBCS* (Sobic.005G042000) and ORF of *SbRAF1*
380 (Sobic.006G269400) were synthesized with 1X FLAG tag and 6X HA tag, respectively (GenScript,
381 Piscataway, NJ). *SbRBCS*-FLAG was subcloned under transcriptional control of the maize RBCS
382 promoter + 5'UTR and the *Panicum virgatum* UBI2 (PvUBI2) terminator. The synthesized
383 *SbRAF1*-HA was subcloned under transcriptional control of the maize NADP-ME promoter and
384 *Panicum virgatum* UBI1 (PvUBI1) terminator. The selectable marker gene *npt*II was subcloned
385 under transcriptional control of the ubiquitin promoter from *Zea mays* and SbHSP16.9
386 terminator from *Sorghum bicolor*. The three expression cassettes were subcloned into a L2
387 construct downstream of an RB7 matrix attachment region (MAR) and upstream of TM2 MAR
388 from *Nicotiana tabacum* serving as insulators and confirmed by Sanger sequencing. The
389 minimal expression construct flanked by MARs was excised from the plasmid backbone using
390 the *I-Sce*1 restriction enzyme and gel purified prior to biolistic transformation into sugarcane.

391 **Generation and PCR confirmation of transgenic sugarcane plants**

392 The linearized, minimal construct containing *SbRBCS*, *SbRAF1* and NPTII cassettes flanked by
393 matrix attachment regions was introduced into sugarcane cv. CPCL02-0926 by biolistic gene
394 transfer as described previously[47]. Briefly, cross-sections of sugarcane leaf whorls above the
395 shoot apical meristem were cultured on a modified Murashige & Skoog medium (MS) with B5
396 vitamins (PhytoTech Labs, KS, USA) supplemented with 3 mg/L of 2,4-Dichloro phenoxy acetic
397 acid (PhytoTech Labs, KS, USA) and maintained at 28 ℃ in the dark for induction of
398 embryogenic callus. For biolistic gene transfer, the minimal expression cassette was coated
399 onto gold particles and introduced into embryogenic calli using biolistic PDS-1000/He delivery
400 system (Bio-Rad, Hercules, CA) as described previously[48]. Following 4 weeks of selection of
401 transformed calli on the medium containing the antibiotic Geneticin®, calli were sub-cultured
402 onto regeneration media (MS media with B5 vitamins, supplemented with 1.86 mg/L of α-
403 Naphthaleneacetic acid/NAA (PhytoTech Labs, KS, USA) and 0.09 mg/L of 6-
404 Benzylaminopurine/BAP (PhytoTech Labs, KS, USA)) and maintained at 28 ℃ incubator with
405 16/8 hr light (100 µmol m^{-2} s^{-1}) and dark cycle. Regenerated shoots were transferred to
406 modified MS basal medium (PhytoTech Labs, KS, USA) for shoot elongation and rooting. Rooted
407 plantlets were transferred to soil and acclimatized in a temperature-controlled growth chamber
408 maintained at 28 ℃ day and 22 ℃ night temperature with 16/8 hr light (400 µmol m^{-2} s^{-1}) and
409 dark cycle for growth and further analysis.

410 For the PCR confirmation of transgenic events, DNA was isolated from 100 mg of leaf tissues
411 using CTAB method with modifications[49]. PCR reactions were performed on a thermocycler
412 (Applied Biosystems, Foster City, CA) using standard Taq buffer, dNTPs and hot start Taq
413 polymerase (New England Biolabs Inc, Ipswich, MA). A construct specific primer (Forward:
414 Primer-1F: 5'- TAATGGTGGTGTAGCTCGACG -3', Reverse: Primer-1R: 5'-
415 TGGCTTGGTTAGGTTTGGCT -3' and marker gene specific primers NPTII_F: 5'-
416 TACCTGCCCATTCGACCACC-3' and 5'-TAAAGCACGAGGAAGCGGTC-3') were used for PCR
417 amplification and yielded 209 bp and 345 bp amplicons, respectively. Amplicons were resolved
418 with electrophoresis on a 1.2% agarose gel and visualized under UV transilluminator (Bio-Rad,
419 Hercules, CA).

420

421 **Plant growth – greenhouse conditions**

422 T2 homozygous *Sorghum bicolor* (inbred RTx430) seeds from 3 independent single insertion
423 events and non-transformed WT seeds from the same harvest date were sowed into plastic
424 potting trays 6 cm x 6 cm x 5.4 cm deep, filled with BM7 growing medium (BM7 All-Purpose
425 Bark Mix, Berger). After about 14 days seedlings were transplanted into 9.5L plastic pots filled
426 with BM7 growing medium supplemented with 44 cm^3 of 13-13-13 (N-P-K) granulated slow-
427 release fertilizer (Osmocote, ICL-Growing Solutions). Sugarcane (*Saccharum officinarum* cv.
428 CPCL02-0926) plantlets clonally propagated from three independent T0 transformation events
429 and non-transformed WT plants were also grown in the greenhouse. Single node segments
430 from mature stalks were transplanted into 9.5L plastic pots filled with BM7 growing medium
431 supplemented with 44 cm^3 of 13-13-13 (N-P-K) granulated slow-release fertilizer. Both sorghum
432 and sugarcane were grown under natural illumination with an additional 350 to 450 µmol $m^{-2}s^{-1}$
433 of LED light. Lights turned on from 6:30am to 9:30pm (15 hour days) and turned off when
434 outside light intensity surpassed 350 watts/m^2 (~800 µmol $m^{-2}s^{-1}$). The greenhouse temperature
435 was kept between 25-28°C in the day and 24-26 °C at night. Both sorghum and sugarcane plants
436 were fertilized with a rotation of 20-10-20 & 15-5-15 liquid fertilizer (JR Peters INC) at 300 ppm
437 N twice a week. Once a month a $MgSO_4$ (100 ppm) and iron (10 ppm) drench was applied
438 (Sprint 138, BASF Corporation).

439 Sugarcane plants were harvested after 2 months of growth. Immediately prior to harvesting,
440 leaf number (fully expanded), tiller number, plant height and stem width were measured. Stem
441 width was measured at the widest point approximately 5 cm above the soil using calipers.
442 Height was measured from the soil to the top of the youngest fully expanded leaf (leaf collar
443 present). Leaf mass per area (LMA) was measured from 3.15 cm^2 of leaf discs, which were dried
444 until constant weight and weight recorded. Chlorophyll content was measured using a SPAD
445 meter (502, Spectrum Technologies). Harvested material was partitioned into main stem
446 biomass and leaf plus tiller biomass and dried at 60°C to steady state weight. Above ground
447 biomass was calculated as the sum of stem, leaf and tiller biomass.

448

449 **Plant growth – field conditions**

450 Sorghum seed obtained from the plants in the greenhouse experiment were harvested and
451 used for a field experiment. A randomized complete block design with six blocks was used. Each
452 block contained 16 rows in a north-south direction, made up of four rows from each of the
453 transgenic lines and WT control (Fig. S4a). Prior to planting the ground was worked with a field
454 cultivator (April 27 2023), and no fertilizer was applied to the soil. Seeds were sowed using a
455 precision planter at a density of 8.6 m^{-2} (Almaco) on June 2nd on the Crop Sciences Farm of the
456 University of Illinois SoyFACE Experimental Station (40°02'36.0"N 88°13'48.5"W). Weather data
457 was collected with an automatic weather station on the Farm (Fig. S4b-d). July 5th Warrior II
458 with Zeon technology (Syngenta) was applied at a moderate rate of 0.07 dm^3/ha for the control
459 of flea beetles. August 2nd Mustang Maxx (FMC Corporation) was applied at moderate rate of
460 0.1 dm^3/ha for the control of aphids.

461 To avoid any release of pollen, paper bags enclosed the panicles, sealed at the peduncle, prior
462 to anthesis, and remaining until harvest. Plants were harvested by hand on October 4th from
463 the middle two rows of each plot by cutting stems at ground level. Two plants from either end
464 of each row were discarded to avoid edge effects. Harvested material was partitioned into
465 stem/leaves and panicles with seed. Stem and leaves were dried to a constant weight in custom
466 made drying ovens at 60°C and panicles with seed were dried at 30°C. Dry weights per block
467 were obtained for both, then seed was collected using a threshing machine (BT 14-E Belt
468 Thresher, Almaco). The machine was cleaned between each sample to avoid contamination.
469 Total seed weight per block was then determined. Above ground biomass was calculated as the
470 sum of stem, leaf, panicle and seed biomass. Harvest index was calculated as seed biomass
471 divided by total above ground biomass. Chlorophyll content was measured using a SPAD meter
472 (502, Spectrum Technologies) on August 30th. LMA was measured August 31st from 6.06 cm^2 of
473 leaf tissue.

474

475 **Transcript and protein expression**

476 Prior to RNA and protein extraction tissue was disrupted and homogenized as described
477 previously[50]. RNA was extracted from 1.9 cm^2 of leaf tissue from the youngest fully expanded
478 leaf of greenhouse and field-grown sorghum, using the NucleoSpin RNA Plant Kit (Macherey-
479 Nagel). 700ul of the lysis buffer was used. RNA quantity and quality was assessed using a
480 NanoDrop (Thermo Fisher Scientific). cDNA was synthesized with Superscript IV VILO Mastermix
481 with ezDNase (Thermo Fisher Scientific). qPCR, primer design and validation were conducted as
482 described in Salesse-Smith et al 2024, with the exception that an anneal temperature of 60C
483 was used for all primer sets. See Table S1 for primer sequences. Primer efficiencies were
484 between 100-105%. Calibrated Normalized Relative Quantities (CNRQ) were calculated using

485 qBase+ software v.3.2 (CellCarta) based on the expression of two reference genes, SbEIF4α and
486 SbActin11.

487 Total protein was extracted from 1.9 cm^2 of leaf tissue from the youngest fully expanded leaf of
488 greenhouse-grown sorghum and sugarcane and field-grown sorghum. Protein extraction and
489 western blots were performed as described previously[50]. The following primary antibodies were
490 used: anti-HA (AS12 2220, Agrisera) at a 1:5000 dilution, anti-LS (AS03 037, Agrisera) at a
491 1:10000 dilution, anti-FLAG (F7425-.2MG, Sigma-Aldrich) at a 1:5000 dilution and anti-RAF1
492 (custom rabbit antibody, Pacific Immunology) at a 1:1000 dilution. For the custom antibody, a
493 23 amino acid immunograde peptide from the maize RAF1 protein (aa 211-233;
494 KGFPRWRGEEGWEAFSKDSPADC) was synthesized and antisera generated by Pacific
495 Immunology.

496

497 **Rubisco content measurements**

498 Leaf discs were sampled from the youngest fully expanded leaves of greenhouse-grown
499 sorghum (1.9 cm^2) and sugarcane (2.5 cm^2) plants, snap-frozen in liquid nitrogen and stored at
500 -80°C. Samples were taken from the same location gas exchange measurements were made the
501 day after measurements were completed. Soluble protein was extracted in 2 ml of N_2-sparged
502 extraction buffer: 50 mM EPPS-NaOH pH 8, 1 mM EDTA, 5 mM $MgCl_2$, 1% (w/v) PVPP, 5 mM
503 DTT and 1% (v/v) protease inhibitor cocktail (P9599, Sigma-Aldrich). Frozen leaf discs were
504 ground in ice-cold Ten Broeck homogenizers (7ml, Corning) containing extraction buffer. Total
505 soluble protein was quantified using the Qubit Protein Assay Kit (Q33211, Life Technologies) on
506 the Qubit 3 Fluorometer (Q33216; Life Technologies). Total Rubisco content was measured by
507 ^{14}C-CABP binding as previously described (Ruuska et al., 1998; Sharwood et al., 2008). 100µl of
508 protein lysate was mixed with an equal volume of Rubisco activation buffer (50 mM EPPS-NaOH
509 pH 8, 1 mM EDTA, 20 mM $MgCl_2$, 30 mM $NaHCO_3$) and let sit at room temperature. After 20
510 minutes, 60µM of ^{14}C-CABP was added to the mixture and left at room temperature for an
511 additional 30 minutes, and then transferred to ice. 100µl of the activated Rubisco protein
512 mixture was loaded onto the size-exclusion chromatography columns and fractions containing
513 ^{14}C-CABP – Rubisco complexes collected. The amount of ^{14}C-CABP was determined by liquid
514 scintillation (Packard Tri-Carb 1900 TR, Canberra Packard Instruments Co). Leaf Rubisco
515 content was calculated as described previously[51].

516

517 **Leaf gas exchange measurements**

518 CO_2 response (A-C_i) and light induction curves were measured on the youngest fully expanded
519 leaves using an infrared gas exchange system LI-6800 fitted with the multiphase flash
520 fluorometer and 6 cm^2 cuvette (6800-01A, LI-COR Environmental). CO_2 response curves were
521 measured simultaneously with chlorophyll fluorescence and used to assess A, C_i, g_{sw}, PhiPSII,

522 $V_{c,max}$ and $V_{p,max}$. A-C_i curves were measured in the field-grown sorghum on July 10th, August 4th
523 and August 29th. Leaves were acclimated to the following conditions: light intensity of 1800
524 µmol m^{-2} s^{-1}, leaf temperature of 30 °C, CO_2 reference concentration of 400 µmol mol^{-1} and 65%
525 humidity. Once A and g_{sw} stabilized, response curves were initiated using the following
526 sequence of reference CO_2 concentrations: 400, 300, 200, 120, 70, 30, 10, 400, 400, 500, 700,
527 900, 1200, and 1500 µmol mol^{-1}. Measurements were logged 3 to 5 minutes after each new CO_2
528 step. A-C_i curves for greenhouse-grown sorghum were measured under the same conditions
529 except for the following changes: a leaf temperature of 28 °C was used and the CO_2 sequence
530 used concentrations of 600 and 800 µmol mol^{-1} CO_2 instead of 700 and 900. Sugarcane A-C_i
531 curves used a CO_2 reference concentration of 450 µmol mol^{-1} and the following sequence of
532 CO_2: 450, 1500, 1250, 1000, 750, 600, 500, 400, 300, 200, 120, 70, 30, and 10 µmol mol^{-1}. $V_{c,max}$
533 and $V_{p,max}$ at 25°C were estimated using the *fit_c4_aci* function from the PhotoGEA R package[52],
534 which fits a mechanistic model to the measured CO_2 response curves[7].

535 Light induction curves were used to assess average A in either the first 180 or 300 seconds since
536 the light was turned on and time to 50% A_{max}, which is determined from the normalized
537 induction curves. Leaves were acclimated to the following conditions: light intensity of 0 µmol
538 m^{-2} s^{-1}, leaf temperature of 28°C (greenhouse-grown sorghum) or 30 °C (field-grown sorghum
539 and sugarcane), CO_2 sample concentration of 400 (sorghum) or 450 µmol mol^{-1} (sugarcane) and
540 65% humidity. After 30 minutes in the dark, light was increased to 1800 µmol m^{-2} s^{-1} and data
541 points logged every 10 s over the course of 30 min. After gas exchange measurements were
542 completed on the greenhouse-grown sorghum plants, leaf number, tiller number and height
543 were recorded.

544

545 **Estimating bundle sheath leakiness using carbon isotope discrimination coupled with leaf gas**
546 **exchange**

547 A LI-6800 gas exchange system (LI-COR Environmental) with the large light source chamber
548 (6800-03) was coupled to a tunable-diode laser absorption spectroscope (TDLAS model TGA
549 200A; Campbell Scientific) to measure online carbon isotope discrimination as described
550 previoulsy[24]. The TDL was connected to the LI-6800 reference air stream using the port on the
551 back of the sensor head, and connected to the sample air stream using the port on the front of
552 the sensor head. CO_2-free air (N_2/O_2) with 21% O_2 was created by mixing two gas streams with
553 mass flow controllers (OMEGA Engineering Inc.). This air supplied the gas exchange system, and
554 was used in the calibration to correct for any drift in the TDL during measurements. The TDL
555 was calibrated using a 2-point calibration where a linear fit is applied using the measurements
556 from two calibration tanks with known [$^{12}CO_2$], [$^{13}CO_2$] (NOAA Global Monitoring Laboratory).
557 The measurements cycled through four gas streams in the following sequence: calibration
558 points 1500 and 100 ppm CO_2 (NOAA Global Monitoring Laboratory), LI-COR 6800 reference air
559 stream, leaf chamber air stream, and reference air stream a second time. Each step had a
560 duration of 30 s, except for the leaf chamber air, which had a duration of 600 s for a total cycle

561 time of 720 s. Measurements were averaged over the last 10 s to produce a single data point
562 for the calibration and reference measurements each cycle. For the sample line, measurements
563 were averaged over 10 s intervals, excluding the first 10 s, to have 59 data points each cycle.

564 The gas exchange system was set to the following conditions: light intensity of 0 µmol m^{-2} s^{-1},
565 leaf temperature of 27°C, flow rate of 300 µmol s^{-1}, 21% O_2, and 800 µmol mol^{-1} CO_2. Once
566 steady-state respiration was reached, five consecutive measurements were logged to measure
567 dark respiration. Afterwards the system was initiated to auto-log at 10s intervals over the
568 course of 30 min. Light intensity increased to 1800 µmol m^{-2} s^{-1} upon initiation of the auto
569 program. Sorghum leaves from the field were cut from plants pre-dawn, submerged in water
570 and brought to the lab where they were re-cut underwater and left in the dark until measured.
571 Only steady state measurements of leakiness were calculated (25-30 min after light turned on).

572 Observed photosynthetic discrimination ($\Delta^{13}C$) was derived and bundle sheath leakiness (ϕ)
573 was subsequently calculated from gas exchange parameters and $\Delta^{13}C$ as described
574 previously[53,54]. Data processing and calculations of $\Delta^{13}C$ and ϕ were done using the MATLAB
575 tool developed previously[24], with minor modifications to apply the 2-point calibration discussed
576 above.

577

578 **Carbon and nitrogen analysis**

579 Leaf tissue from field grown sorghum was oven dried to a constant weight, ground and total
580 carbon (C), C isotope analysis (δ15C), total nitrogen (N), and N isotope analysis (δ15N)
581 measured using an elemental analyzer (Costech Elemental Combustion System 4010, Costech
582 Analytical Technologies) coupled with a continuous flow isotope ratio mass spectrometer
583 (DeltaV Advantage, Thermo Fisher Scientific). Spinach leaves (National Institute of Standards
584 and technology Standard Reference Material 1570a) and acetanilide (USA Analytical) were used
585 as standards for C and N analysis. Isotope analysis was measured relative to the international
586 standards NBS 19 for C ($\delta^{13}C_{V\text{-}PDB}$ = 1.95‰) and atmospheric N_2 for N ($\delta^{15}N_{Air}$ = 0‰).

587

588 **Statistical analysis**

589 Normality of the data was tested with Shapiro-Wilk's test, and homoscedasticity with Brown-
590 Forsythe's test. If criteria for normal distributions and equal variance was met one-way ANOVA
591 followed by Dunnett's *post hoc* test for transgenic mean comparison against the WT control
592 was performed. Data were considered significant at $P < 0.05$. If criteria for normality was
593 violated Wilcoxon's non-parametric test was applied. Analysis of field growth traits (Fig. 4) was
594 performed using a randomized block design with 6 blocks. Tests used are indicated in the figure
595 or table legend. Jmp pro version 17.0.0 software was used for all statistical analyses.

596

Acknowledgements

We thank Monty Flack for maintenance of the greenhouse plants. We thank David Drag, Ben Thompson, and Andy Wszalek for help with the maintenance of the sorghum field experiment and field harvest. We thank Edward Lochocki for assistance during field work and Samantha Stutz for maintenance of the TDL. We also thank Mike Masters and Chuck Hyde for performing the C and N analysis and Ben Haas for initial help with plasmid assembly. This work was funded by the DOE Center for Advanced Bioenergy and Bioproducts Innovation (U.S. Department of Energy, Office of Science, Biological and Environmental Research Program under Award Number DE-SC0018420). Any opinions, findings, and conclusions or recommendations expressed in this publication are those of the author(s) and do not necessarily reflect the views of the U.S. Department of Energy.

Conflict of Interest

The authors declare no conflicts of interest.

Author Contributions

CES and SPL conceived of and designed the experiments. TEC coordinated sorghum transformation, MG assembled the vector and ZG generated and confirmed the transgenic sorghum lines. FA coordinated sugarcane transformation, BK and TN, generated and confirmed the transgenic sugarcane lines. NA and CES assembled the recombinant DNA vector for sugarcane, and performed experimental measurements. CES analyzed the data. CES and SPL wrote the manuscript with contributions and review from all authors.

Supporting Information

Fig. S1: Gene expression in greenhouse and field grown sorghum.
Fig. S2: Normalized induction curves from greenhouse and field grown sorghum.
Fig. S3: Plant growth traits in greenhouse grown sorghum plants.
Fig. S4: Sorghum field experimental design and weather conditions.
Fig. S5: Steady-state BS leakiness of field grown sorghum.
Fig. S6: Normalized induction curves from greenhouse-grown sugarcane.
Fig. S7: Plant growth traits in greenhouse grown sugarcane plants.
Fig. S8: Average yield of sorghum and sugarcane over the last 20 to 30 years.
Table S1: qPCR primer information
Table S2: Summary of leaf mass per area (LMA), chlorophyll content (SPAD value), total soluble protein (TSP) and harvest measurements of sorghum and sugarcane plants.

633 **Table 1. Summary of leaf gas exchange measurements from greenhouse grown sorghum and**
634 **sugarcane.** Values are shown as the mean ± SEM. Values significantly different from WT at $P < 0.05$ are
635 in bold. One-way ANOVA, Dunnett's post hoc test.

Parameter	WT	RBCS-RAF1 Hn1a	RBCS-RAF1 Zg12a	RBCS-RAF1 Zg5b	Sample number (*N*)
Sorghum - Greenhouse					
ΦPSII	0.299 ± 0.002	**0.336 ± 0.007**	**0.331 ± 0.009**	**0.338 ± 0.006**	7-10
$V_{p,max}$ ($\mu mol\ m^{-2}\ s^{-1}$)	80.32 ± 7.38	88.33 ± 3.19	88.05 ± 3.59	89.99 ± 2.93	7-10
C_i ($\mu mol\ mol^{-1}$)	153.53 ± 2.36	142.53 ± 2.18	144.62 ± 3.55	144.50 ± 4.95	7-10
g_{sw} ($mol\ m^{-2}\ s^{-1}$)	0.411 ± 0.010	**0.463 ± 0.009**	**0.472 ± 0.012**	**0.472 ± 0.014**	7-10
Parameter	WT	RBCS-RAF1 3	RBCS-RAF1 9	RBCS-RAF1 25	Sample number (*N*)
Sugarcane - Greenhouse					
ΦPSII	0.297 ± 0.012	0.319 ± 0.008	0.300 ± 0.009	0.326 ± 0.009	10
$V_{p,max}$ ($\mu mol\ m^{-2}\ s^{-1}$)	68.82 ± 4.55	85.70 ± 6.97	68.99 ± 3.02	79.93 ± 4.76	9-10
C_i ($\mu mol\ mol^{-1}$)	116.48 ± 8.61	113.76 ± 6.29	121.17 ± 4.47	118.55 ± 3.27	9-10
g_{sw} ($mol\ m^{-2}\ s^{-1}$)	0.252 ± 0.012	0.282 ± 0.006	0.282 ± 0.007	**0.305 ± 0.015**	9-10
$\bar{A}_{300}$ ($\mu mol\ m^{-2}\ s^{-1}$)	11.05 ± 2.26	17.78 ± 2.08	5.62 ± 1.95	15.38 ± 1.77	7-8
Time to 50% A_{MAX} (min)	3.36 ± 0.38	3.05 ± 0.27	**9.27 ± 1.62**	3.35 ± 0.26	6-8

636
637
638
639
640
641
642
643
644

References

1 FAO. *FAOSTAT*, <https://www.fao.org/faostat/en/#data> (2024).

2 Healey, A. L. *et al.* The complex polyploid genome architecture of sugarcane. *Nature*, doi:10.1038/s41586-024-07231-4 (2024).

3 Dohleman, F. G. & Long, S. P. More Productive Than Maize in the Midwest: How Does Miscanthus Do It? *Plant Physiology* **150**, 2104-2115, doi:10.1104/pp.109.139162 (2009).

4 He, Y., Jaiswal, D., Long, S. P., Liang, X.-Z. & Matthews, M. L. Biomass yield potential on U.S. marginal land and its contribution to reach net-zero emission. *GCB Bioenergy* **16**, e13128, doi:https://doi.org/10.1111/gcbb.13128 (2024).

5 Heaton, E. A., Dohleman, F. G. & Long, S. P. Meeting US biofuel goals with less land: the potential of Miscanthus. *Global Change Biology* **14**, 2000-2014, doi:10.1111/j.1365-2486.2008.01662.x (2008).

6 Matsuoka, S., Kennedy, A. J., Santos, E. G. D. d., Tomazela, A. L. & Rubio, L. C. S. Energy Cane: Its Concept, Development, Characteristics, and Prospects. *Advances in Botany* **2014**, 597275, doi:10.1155/2014/597275 (2014).

7 von Caemmerer, S. Updating the steady-state model of C4 photosynthesis. *Journal of Experimental Botany* **72**, 6003-6017, doi:10.1093/jxb/erab266 (2021).

8 Walker, B. J., VanLoocke, A., Bernacchi, C. J. & Ort, D. R. The Costs of Photorespiration to Food Production Now and in the Future. *Annual Review of Plant Biology* **67**, 107-127, doi:10.1146/annurev-arplant-043015-111709 (2016).

9 Ermakova, M. *et al.* Installation of C4 photosynthetic pathway enzymes in rice using a single construct. *Plant Biotechnology Journal* **19**, 575-588, doi:10.1111/pbi.13487 (2021).

10 Furbank, R., Kelly, S. & von Caemmerer, S. Photosynthesis and food security: the evolving story of C4 rice. *Photosynthesis Research* **158**, 121-130, doi:10.1007/s11120-023-01014-0 (2023).

11 Bianconi, M. E. *et al.* Continued adaptation of C4 photosynthesis after an initial burst of changes in the Andropogoneae grasses. *Systematic Biology* **69**, 445-461, doi:10.1093/sysbio/syz066 (2019).

12 Ainsworth, E. A. & Long, S. P. What have we learned from 15 years of free-air CO2 enrichment (FACE)? A meta-analytic review of the responses of photosynthesis, canopy. *New Phytologist* **165**, 351-371, doi:doi:10.1111/j.1469-8137.2004.01224.x (2005).

13 Ainsworth, E. A. & Long, S. P. 30 years of free-air carbon dioxide enrichment (FACE): What have we learned about future crop productivity and its potential for adaptation? *Global Change Biology* **26**, 27-49, doi:doi:10.1111/gcb.15375 (2020).

14 Leakey, A. D. B., Bernacchi, C. J., Dohleman, F. G., Ort, D. R. & Long, S. P. Will photosynthesis of maize (Zea mays) in the US Corn Belt increase in future CO2 rich atmospheres? An analysis of diurnal courses of CO2 uptake under free-air concentration enrichment (FACE). *Global Change Biology* **10**, 951-962, doi:10.1111/j.1365-2486.2004.00767.x (2004).

15 Leakey, A. D. B. *et al.* Photosynthesis, productivity, and yield of maize are not affected by open-air elevation of CO2 concentration in the absence of drought. *Plant Physiology* **140**, 779-790, doi:10.1104/pp.105.073957 (2006).

16 de Souza, A. P., Arundale, R. A., Dohleman, F. G., Long, S. P. & Buckeridge, M. S. Will the exceptional productivity of Miscanthus x giganteus increase further under rising atmospheric CO2? *Agricultural and Forest Meteorology* **171**, 82-92, doi:10.1016/j.agrformet.2012.11.006 (2013).

17 Sage, R. F. & Kubien, D. S. Quo vadis C4? An ecophysiological perspective on global change and the future of C4 plants. *Photosynth Res* **77**, 209-225, doi:10.1023/a:1025882003661 (2003).

18 Furbank, R. T. Walking the C4 pathway: past, present, and future. *Journal of Experimental Botany* **67**, 4057-4066, doi:10.1093/jxb/erw161 (2016).

19 Pignon, C. P. & Long, S. P. Retrospective analysis of biochemical limitations to photosynthesis in 49 species: C4 crops appear still adapted to pre-industrial atmospheric [CO2]. *Plant, Cell & Environment* **43**, 2606-2622, doi:https://doi.org/10.1111/pce.13863 (2020).

20 von Caemmerer, S. & Furbank, R. T. Strategies for improving C4 photosynthesis. *Current Opinion in Plant Biology* **31**, 125-134, doi:10.1016/j.pbi.2016.04.003 (2016).

21 NOAA. *Trends in Atmospheric Carbon Dioxide*, <https://gml.noaa.gov/ccgg/trends/global.html> ((2024).

22 Ahn, J. *et al.* A record of atmospheric CO2 during the last 40,000 years from the Siple Dome, Antarctica ice core. *Journal of Geophysical Research: Atmospheres* **109**, D13305, doi:https://doi.org/10.1029/2003JD004415 (2004).

23 Wang, Y., Chan, K. X. & Long, S. P. Towards a dynamic photosynthesis model to guide yield improvement in C4 crops. *The Plant Journal* **107**, 343-359, doi:https://doi.org/10.1111/tpj.15365 (2021).

24 Wang, Y. *et al.* Increased bundle-sheath leakiness of CO2 during photosynthetic induction shows a lack of coordination between the C4 and C3 cycles. *New Phytologist* **236**, 1661-1675, doi:10.1111/nph.18485 (2022).

25 Furbank, R. T. *et al.* Genetic Manipulation of Key Photosynthetic Enzymes in the C4 plant Flaveria bidentis. *Functional Plant Biology* **24**, 477-485, doi:https://doi.org/10.1071/PP97028 (1997).

26 Salesse-Smith, C. E. *et al.* Overexpression of Rubisco subunits with RAF1 increases Rubisco content in maize. *Nature Plants* **4**, 802-810, doi:10.1038/s41477-018-0252-4 (2018).

27 Salesse-Smith, C. E., Sharwood, R. E., Busch, F. A. & Stern, D. B. Increased Rubisco content in maize mitigates chilling stress and speeds recovery. *Plant Biotechnology Journal* **18**, 1409-1420, doi:10.1111/pbi.13306 (2020).

28 Yoon, D. K. *et al.* Transgenic rice overproducing Rubisco exhibits increased yields with improved nitrogen-use efficiency in an experimental paddy field. *Nature Food* **1**, 134-139, doi:10.1038/s43016-020-0033-x (2020).

29 Long, S. P. *et al.* Into the Shadows and Back into Sunlight: Photosynthesis in Fluctuating Light. *Annual Review of Plant Biology* **73**, 617-648, doi:10.1146/annurev-arplant-070221-024745 (2022).

30 Slattery, R. A., Walker, B. J., Weber, A. P. M. & Ort, D. R. The Impacts of Fluctuating Light on Crop Performance. *Plant Physiology* **176**, 990-1003, doi:10.1104/pp.17.01234 (2018).

31 Feller, U., Anders, I. & Mae, T. Rubiscolytics: fate of Rubisco after its enzymatic function in a cell is terminated. *Journal of Experimental Botany* **59**, 1615-1624, doi:10.1093/jxb/erm242 (2007).

32 Flamholz, A. I. *et al.* Revisiting Trade-offs between Rubisco Kinetic Parameters. *Biochemistry* **58**, 3365-3376, doi:10.1021/acs.biochem.9b00237 (2019).

33 Sage, R. F. & McKown, A. D. Is C4 photosynthesis less phenotypically plastic than C3 photosynthesis? *Journal of Experimental Botany* **57**, 303-317, doi:10.1093/jxb/erj040 (2005).

34 Pignon, C. P., Lundgren, M. R., Osborne, C. P. & Long, S. P. Bundle sheath chloroplast volume can house sufficient Rubisco to avoid limiting C4 photosynthesis during chilling. *Journal of Experimental Botany* **70**, 357-365, doi:10.1093/jxb/ery345 (2018).

35 Zhang, G. *et al.* The reference genome of Miscanthus floridulus illuminates the evolution of Saccharinae. *Nature Plants* **7**, 608-618, doi:10.1038/s41477-021-00908-y (2021).

36 Sage, R. F. Was low atmospheric CO_2 during the Pleistocene a limiting factor for the origin of agriculture? *Global Change Biology* **1**, 93-106, doi:10.1111/j.1365-2486.1995.tb00009.x (1995).

37 Wostrikoff, K. & Stern, D. Rubisco large-subunit translation is autoregulated in response to its assembly state in tobacco chloroplasts. *Proc Natl Acad Sci U S A* **104**, 6466-6471, doi:10.1073/pnas.0610586104 (2007).

38 Salvatori, N., Alberti, G., Muller, O. & Peressotti, A. Does Fluctuating Light Affect Crop Yield? A Focus on the Dynamic Photosynthesis of Two Soybean Varieties. *Frontiers in Plant Science* **13**, 862275, doi:10.3389/fpls.2022.862275 (2022).

39 Kromdijk, J. *et al.* Improving photosynthesis and crop productivity by accelerating recovery from photoprotection. *Science* **354**, 857-861, doi:10.1126/science.aai8878 (2016).

40 Taylor, S. H. *et al.* Faster than expected Rubisco deactivation in shade reduces cowpea photosynthetic potential in variable light conditions. *Nature Plants* **8**, 118-124, doi:10.1038/s41477-021-01068-9 (2022).

41 Taylor, S. H. & Long, S. P. Slow induction of photosynthesis on shade to sun transitions in wheat may cost at least 21% of productivity. *Philos Trans R Soc Lond B Biol Sci* **372**, 1730, doi:10.1098/rstb.2016.0543 (2017).

42 Deschamps, S. *et al.* A chromosome-scale assembly of the sorghum genome using nanopore sequencing and optical mapping. *Nature Communications* **9**, 4844, doi:10.1038/s41467-018-07271-1 (2018).

43 Belide, S., Vanhercke, T., Petrie, J. R. & Singh, S. P. Robust genetic transformation of sorghum (Sorghum bicolor L.) using differentiating embryogenic callus induced from immature embryos. *Plant Methods* **13**, 109, doi:10.1186/s13007-017-0260-9 (2017).

44 Miller, F. R. Registration of RTX430 sorghum parental line. *Crop Science* **24**, 1224-1224, doi:10.2135/cropsci1984.0011183X002400060074x (1984).

45 Sheen, J. Metabolic repression of transcription in higher plants. *The Plant Cell* **2**, 1027-1038, doi:10.1105/tpc.2.10.1027 (1990).

46 Guo, X. M., Ge, Z. X., Sato, S. J. & Clemente, T. E. in *Agrobacterium Protocols, Vol 1, 3rd Edition* Vol. 1223 *Methods in Molecular Biology* (ed K. Wang) 181-188 (2015).

47 Taparia, Y., Gallo, M. & Altpeter, F. Comparison of direct and indirect embryogenesis protocols, biolistic gene transfer and selection parameters for efficient genetic transformation of sugarcane. *Plant Cell, Tissue and Organ Culture (PCTOC)* **111**, 131-141, doi:10.1007/s11240-012-0177-y (2012).

48 Altpeter, F. & Sandhu, S. in *Plant Cell Culture: Essential Methods* (eds M Davey & P Anthony) 217-239 (Wiley, 2010).

49 Murray, M. G. & Thompson, W. F. Rapid isolation of high molecular weight plant DNA. *Nucleic Acids Res* **8**, 4321-4325, doi:10.1093/nar/8.19.4321 (1980).

50 Salesse-Smith, C. *et al.* Greater leaf photosynthesis in the field by increasing mesophyll conductance via modified cell wall porosity and thickness in tobacco. *bioRxiv*, 2024.2002.2013.580201, doi:10.1101/2024.02.13.580201 (2024).

51 Whitney, S. M. & Sharwood, R. E. in *Chloroplast Biotechnology: Methods and Protocols* (ed Pal Maliga) 195-214 (Springer US, 2021).

52 Lochocki, E. B. *PhotoGEA: Photosynthetic Gas Exchange Analysis. v.0.11.0*, (2024).

53 Evans, J. R., Sharkey, T. D., Berry, J. A. & Farquhar, G. D. Carbon isotope discrimination measured concurrently with gas-exchange to investigate CO2 diffusion in leaves of higher-plants. *Australian Journal of Plant Physiology* **13**, 281-292, doi:10.1071/pp9860281 (1986).

54 von Caemmerer, S., Ghannoum, O., Pengelly, J. J. L. & Cousins, A. B. Carbon isotope discrimination as a tool to explore C4 photosynthesis. *Journal of Experimental Botany* **65**, 3459-3470, doi:10.1093/jxb/eru127 (2014).